

Supporting Information

APTES functionalization in SBA-15: effect on SO₂ capture and detection applications

Juan L. Obeso,^{a,b,*} Valeria B. López Cervantes,^{b,*} Catalina V. Flores,^{a,b} Celene García-Carvajal,^c Carlos E Garduño-Albino,^e Ricardo A. Peralta,^e Víctor M. Trejos,^d L. Huerta Arcos,^f Illich A. Ibarra,^{b,g} Diego Solis-Ibarra,^b Salomón Cordero-Sánchez,^{d*} Nora S. Portillo-Vélez^{e*} and J. Marcos Esparza-Schulz^{d*}

^a Instituto Politécnico Nacional, CICATA U. Legaria, Laboratorio Nacional de Ciencia, Tecnología y Gestión Integrada del Agua (LNAqua), Legaria 694, Irrigación, 11500, Miguel Hidalgo, CDMX, México.

^b Laboratorio de Fisicoquímica y Reactividad de Superficies (LaFReS), Instituto de Investigaciones en Materiales, Universidad Nacional Autónoma de México, Circuito Exterior s/n, CU, Coyoacán, 04510, Ciudad de México, México.

^c Laboratorio de Sólidos Porosos (LabSoP) - INFAP-CONICET, Universidad Nacional de San Luis, San Luis, Argentina.

^d Laboratorio de Fisicoquímica de Superficies, Departamento de Química, Universidad Autónoma Metropolitana-Iztapalapa, Avenida San Rafael Atlixco 186, Leyes de Reforma 1ra Sección, Iztapalapa, Ciudad de México 09310, Mexico

^e Departamento de Química, División de Ciencias Básicas e Ingeniería, Universidad Autónoma Metropolitana (UAM-I), 09340 México City, México

^f Instituto de Investigaciones en Materiales, Universidad Nacional Autónoma de México, Circuito Exterior Ciudad Universitaria, Coyoacán, 04510, Ciudad de México, México.

^g On Sabbatical as “Catedra Dr. Douglas Hugh Everett” at Departamento de Química, Universidad Autónoma Metropolitana-Iztapalapa, Avenida San Rafael Atlixco 186, Leyes de Reforma 1ra Sección, Iztapalapa, Ciudad de México 09310, Mexico.

* These authors contributed equally to this work.

Table of contents

S1. Experimental details	S3
S2. Characterization	S3
S3. SO ₂ adsorption experiments	S5
S4. SO ₂ selectivity	S8
S5. Custom ex-situ gas adsorption system	S9
S6. Florescence experiments	S10
S7. XPS experiments	S12
S8. DFT calculations	S14
S9. References	S27

S1. Experimental details

Analytical instruments

Powder X-ray diffraction (PXRD) patterns were recorded on a Rigaku Diffractometer, Ultima IV with a Cu-K α_1 radiation ($\lambda = 1.5406 \text{ \AA}$) using a nickel filter. Patterns were recorded in the 5-40° 2θ range with a step scan of 0.02° and a scan rate of 0.08° min $^{-1}$.

Fourier-transform infrared spectroscopy (FT-IR) were obtained in the 4000-500 cm $^{-1}$ range on a Shimadzu IRTtracer-100 spectrometer with a Golden Gate Single Reflection diamond ATR cell.

Time-resolved photoluminescence (TRPL) spectra were measured in an Edinburgh Instruments FS5 Spectrofluorometer using a 335.6 nm EPLED, with an excitation bandwidth of 0.01 nm and an emission bandwidth of 7 nm, at an emission wavelength of 455 nm.

X-ray photoelectron spectroscopy (XPS) was recorded with an ultra-high vacuum (UHV) system Scanning XPS microprobe PHI 5000 VersaProbe II, with a monochromatic X-ray source ($h=1486.6 \text{ eV}$) with 100 μm beam diameter and an MCD analyzer. The C 1s line at 284.8 eV was used as a reference for the binding energy calibration.

S2. Characterization

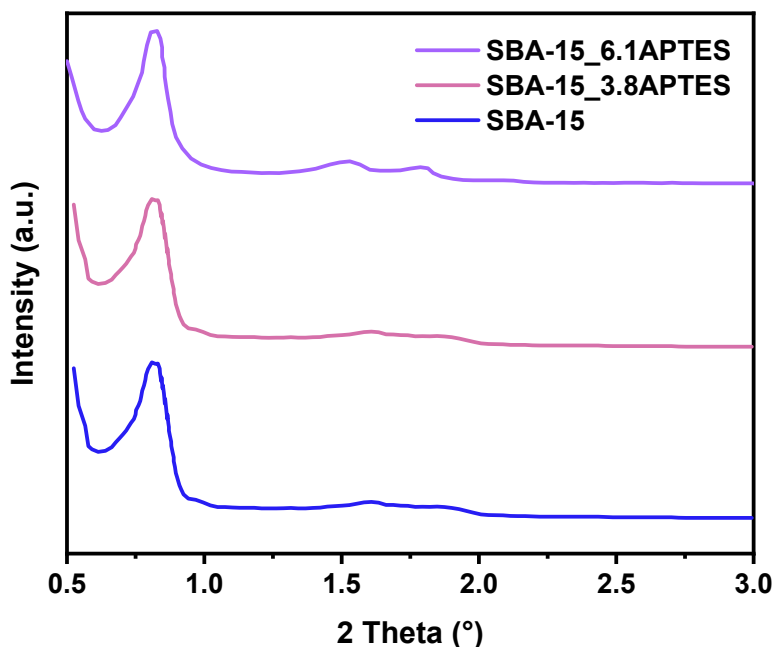


Figure S1. PXRD pattern of SBA-15, SBA-15_3.8APTES, and SBA-15_6.1APTES.

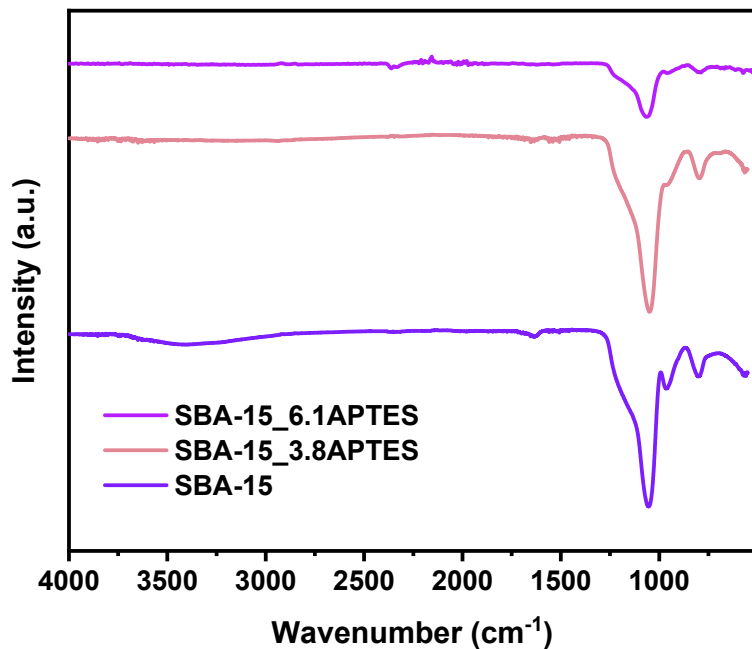


Figure S2. IR spectrum of SBA-15, SBA-15_3.8APTES, and SBA-15_6.1APTES.

Table S1. Elemental analysis by CHN of SBA-15_3.8APTES and SBA-15_6.1APTES

Sample	C (%)	H (%)	N (%)
SBA-15_3.8APTES	3.95	1.05	1.35
SBA-15_6.1APTES	6.41	1.61	2.17

S3. SO₂ adsorption experiments

Comparison of SO₂ adsorption performance of SBA-15 materials.

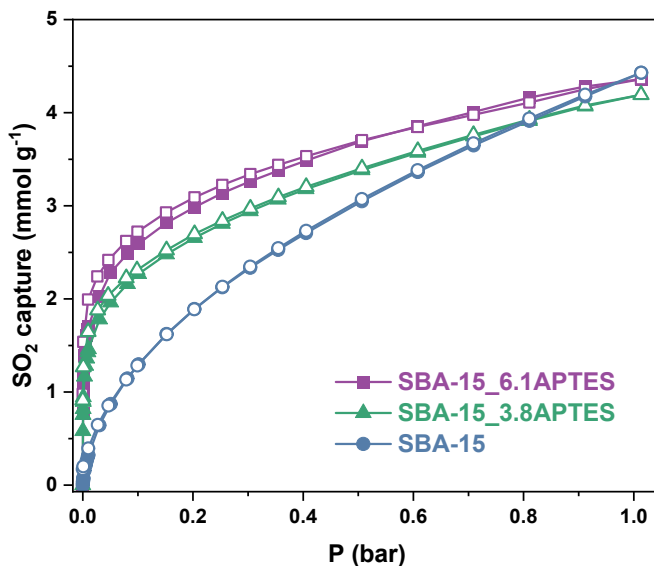


Figure S3. Comparison of SO₂ adsorption-desorption isotherms of SBA-15_6.1APTES (purple), SBA-15_3.8APTES (green), and SBA-15 (blue) at 298 and 1 bar.

Table S2. Comparison of SO₂ adsorption with representative materials

Material	SO ₂ adsorption at 1 bar (mmol g ⁻¹)	Temperature (K)	Ref.
SBA-15	4.43	298	This work
SBA-15_6.1APTES	4.44	298	
SBA-15_3.8APTES	4.19	298	
SBA_WLS-PTA	15.43	298	1
SBA_RS-PTA	14.67	298	
SBA_CS-PTA	14.05	298	
SBA-15PL-mG2	2.07	298	2
SBA-15PL-mG3	2.35	298	
SBA-15PL-mPEI	1.71	298	

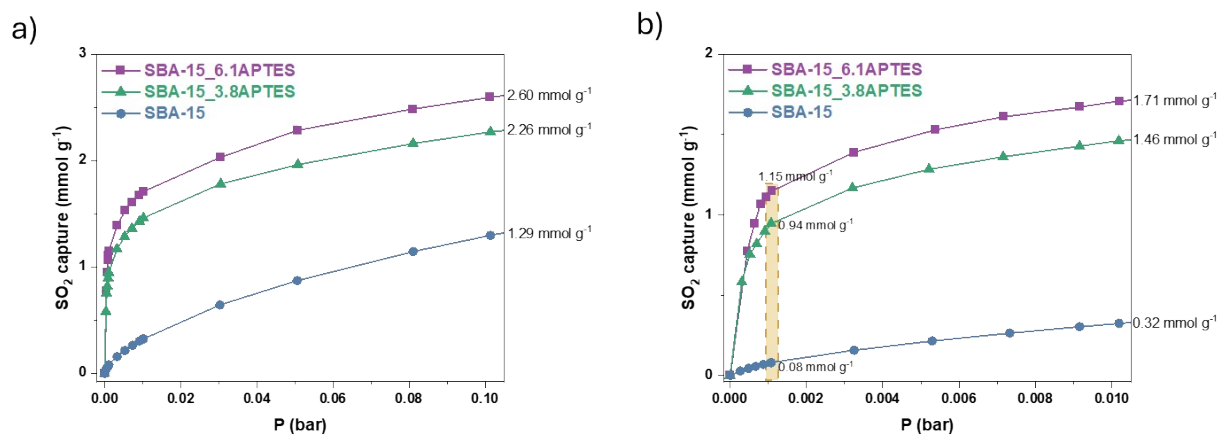


Figure S4. Comparison of SO_2 adsorption-desorption isotherms of SBA-15_6.1APTES (purple), SBA-15_3.8APTES (green) and SBA-15 (blue) at 298 K and a) up to 0.1 bar, and b) up to 0.01 bar.

Recyclability of SBA-15_6.1APTES upon SO_2

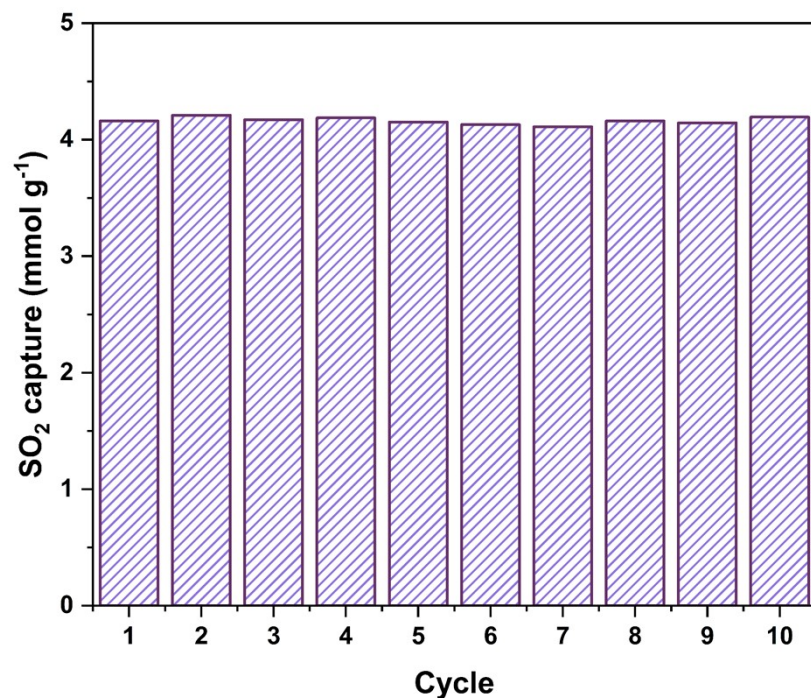


Figure S5. SO_2 adsorption-desorption cycles at 298 K and 0.8 bar.

Stability of SBA-15_6.1APTES after SO_2 adsorption

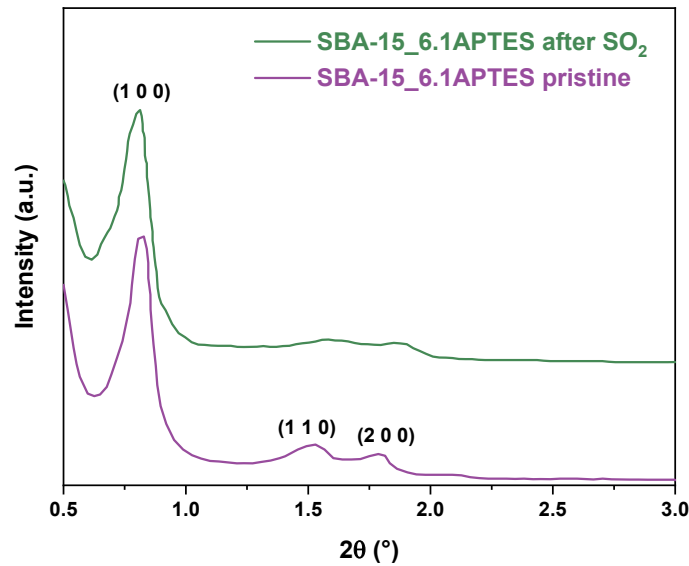


Figure S6. Comparison of PXRD patterns of SBA-15_6.1APTES before (purple) and after (green) after SO_2 adsorption-desorption cycles.

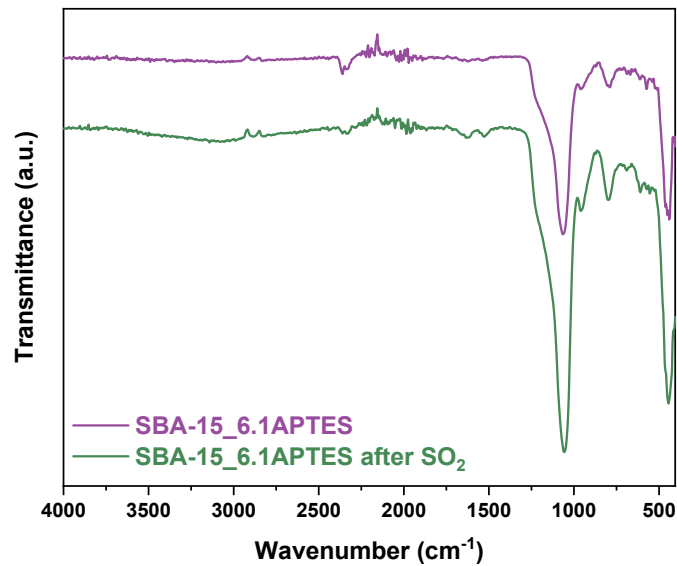


Figure S7. Comparison of FTIR spectra of SBA-15_6.1APTES before (purple) and after (green) after SO_2 adsorption-desorption cycles.

S4. SO₂ selectivity

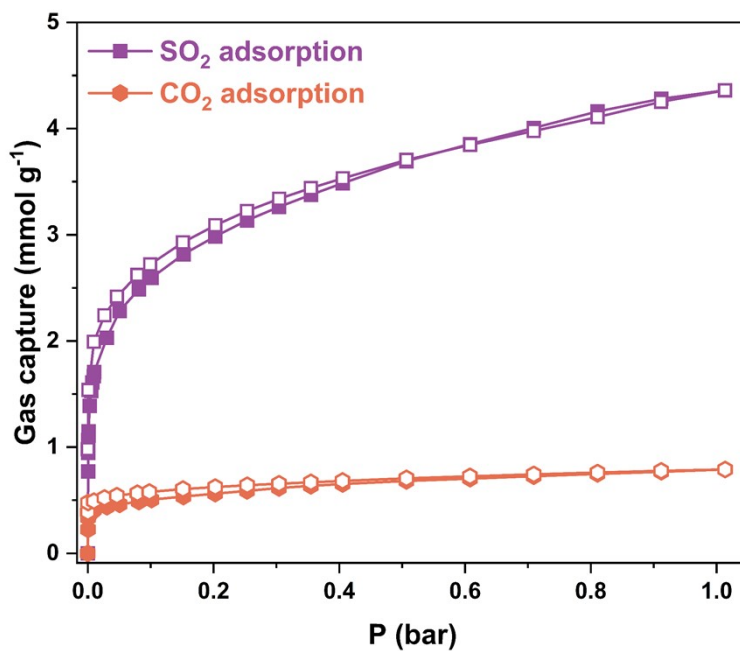


Figure S8. Comparison of mono-component SO₂ (purple) and CO₂ (orange) adsorption-desorption isotherms of SBA-15_6.1APTES.

Predictions of the co-adsorption of SO₂:CO₂ mixtures on SBA and SBA_APTEs were performed assuming the Ideal Adsorbed Solution Theory (IAST) assumptions as valid and using the Python package pylIAST. None of the analytical models available in pylIAST fitted both experimental SO₂ and CO₂ isotherms of SBA and SBA_6.1APTES. Therefore, these adsorption data were linearly interpolated, and the distributed pressures were calculated by numerical quadrature implemented in pylIAST (Figure S9). Therefore, the adsorption selectivity was calculated as:

$$S_{SO_2/CO_2} = \frac{x_{SO_2}/y_{CO_2}}{P_{SO_2}/P_{CO_2}}$$

where x_i and y_i are the mole fraction of components $i = SO_2$ and CO_2 in adsorbed and gas phase, respectively.

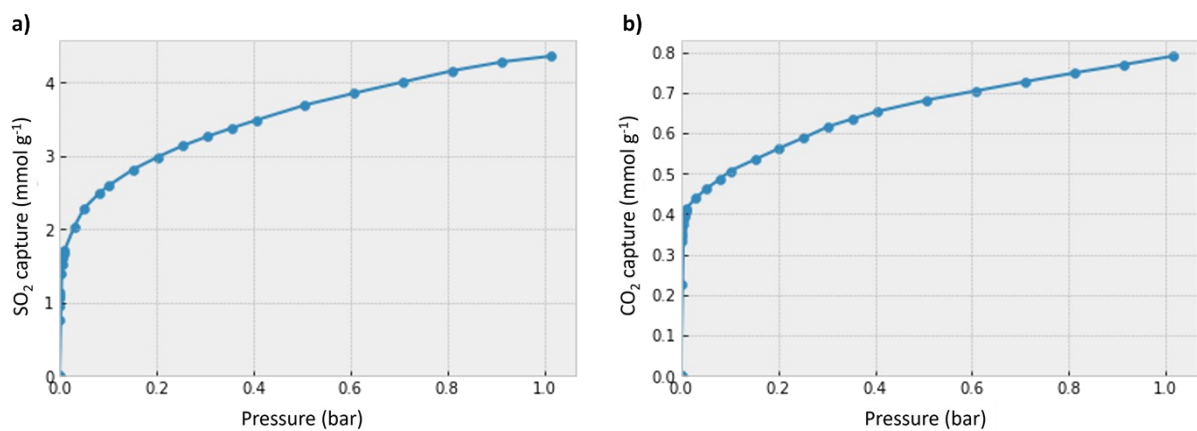


Figure S9. Adsorption isotherms of a) SO_2 and b) CO_2 from SBA-15_6.1APTES at 298 K. The filled circles are the experimental data, while the solid line represents the fit of the interpolation model.

The selectivity of SO_2 versus CO_2 of different SO_2/CO_2 mole fractions at 1 bar pressure was calculated and compared with other porous materials. The results are shown in Table S3.

Table S3. Comparison SO_2 selectivity of SBA-15_6.1APTES and other materials.

	SO ₂ /CO ₂ molar ratio					Ref
	0.001/0.999	0.005/0.995	0.01/0.99	0.05/0.95	0.1/0.9	
SBA-15_6.1APTES	154.48	132.73	123.96	148.45	257.23	This work
SBA-15		41.33	33.17	20.81	18.71	S2
Zeolite Y			265		180	S3
HKUST-1			41		36	S3
SIFSIX-2-Cu-i					87	S4

S5. Custom ex-situ SO_2 adsorption system

The system (Figure S10) contains two principal parts:

- The gas generator, in which Na_2SO_3 is added to a two-neck ball flask [1], one of which is capped with a rubber stopper through which concentrated H_2SO_4 is injected with a glass syringe [2], while the other is connected to the saturation chamber.
- The saturation chamber, made of a round flask [3], is connected to a vacuum line [4] and a pressure gauge [5].

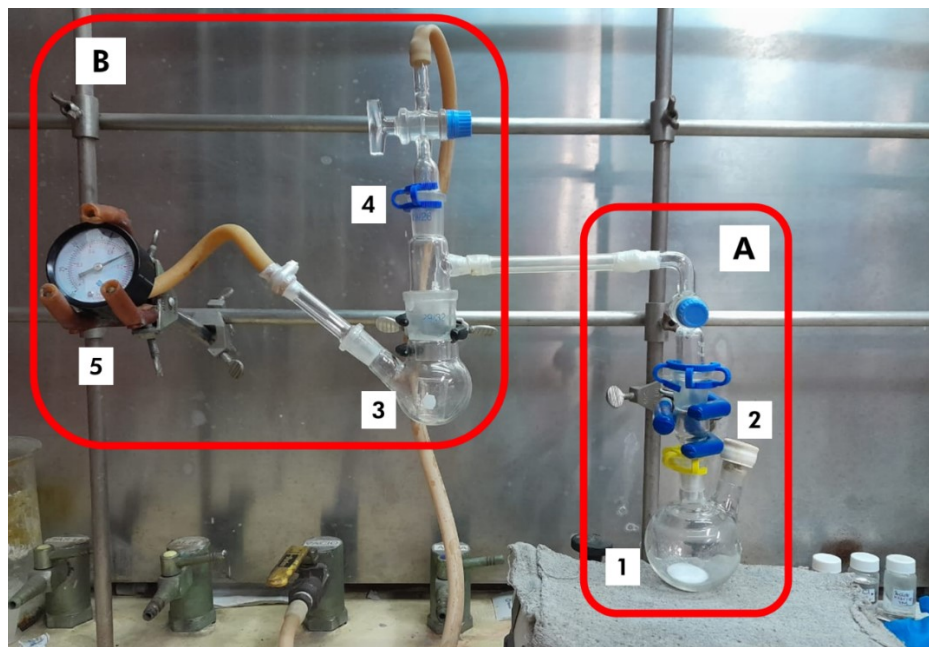


Figure S10. Ex situ SO₂ homemade system.

S6. Florescence experiments

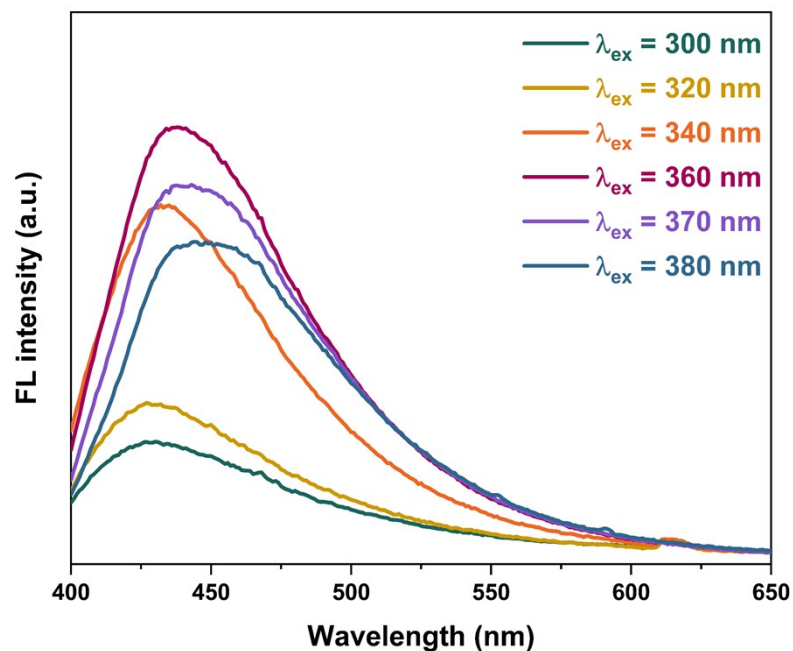


Figure S11. Solid-state emission spectra of activated SBA-15_6.1APTES at different excitation wavelength.

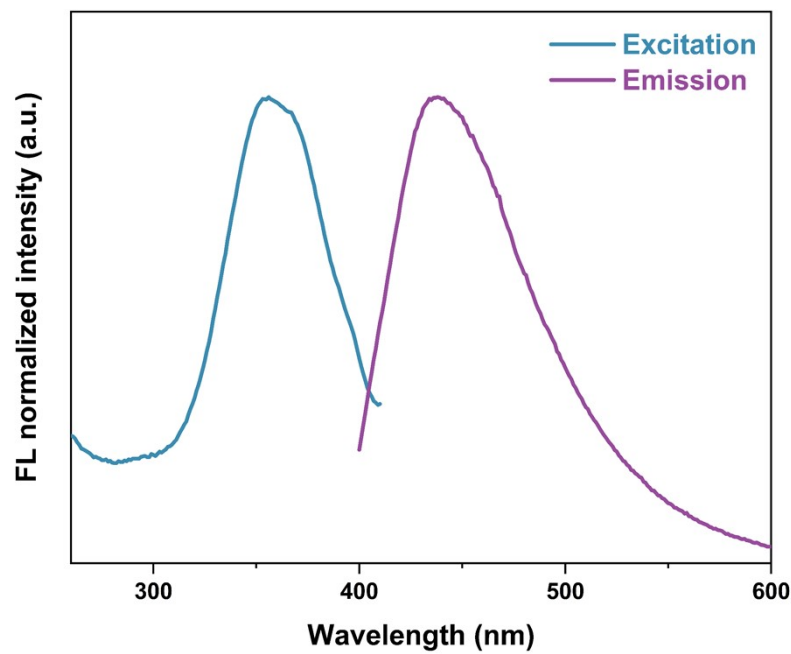


Figure S12. Solid-state excitation (blue) and emission (purple) spectra of activated SBA-15_6.1APTES.

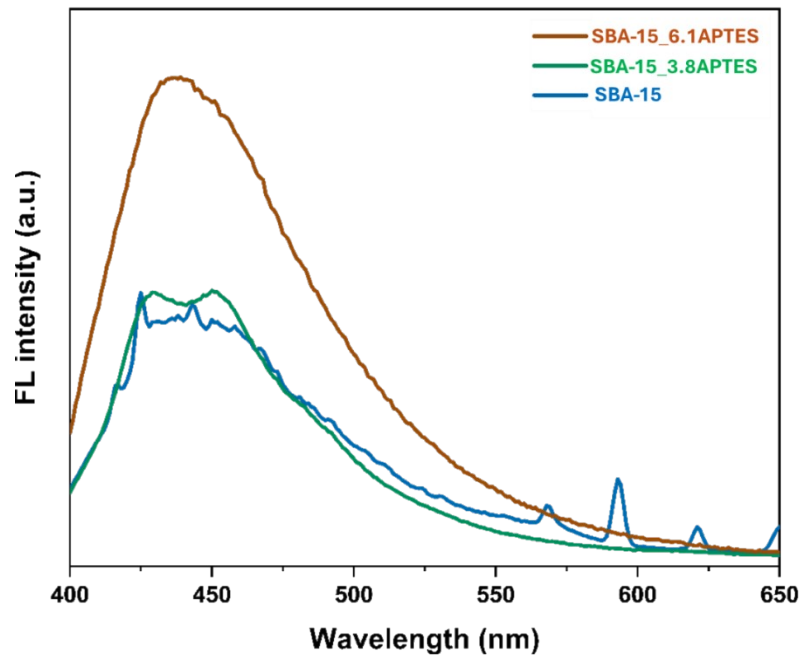


Figure S13. Comparison of the solid-state emission spectra of pristine samples of SBA-15_6.1APTES (brown), SBA-15_3.8APTES (green) and SBA-15 (blue).

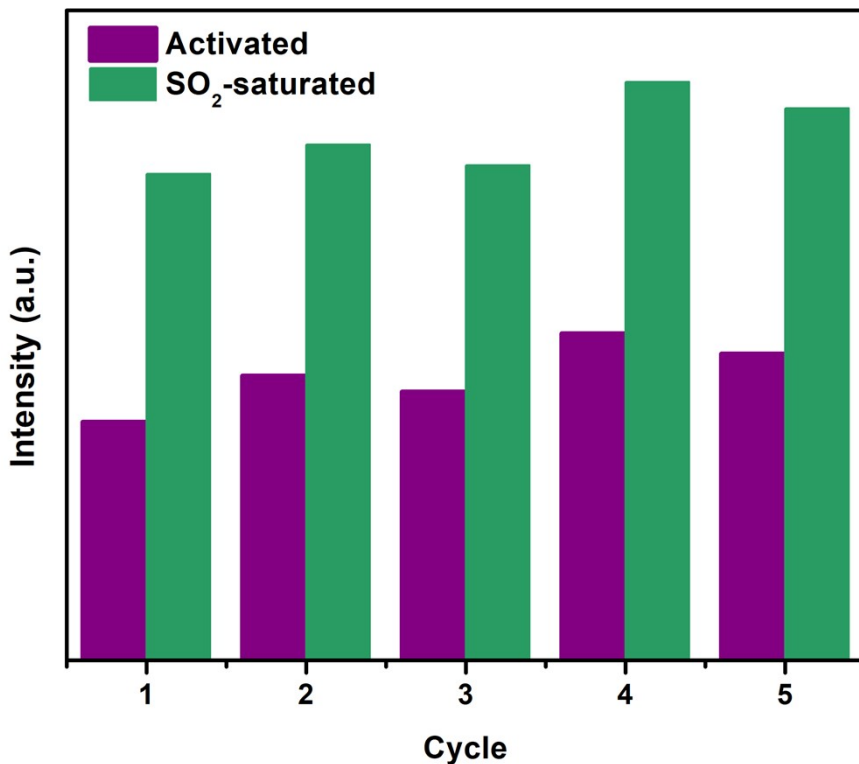


Figure S14. Fluorescence cycles of activated sample and SO_2 -saturated SBA-15_6.1APTES samples.

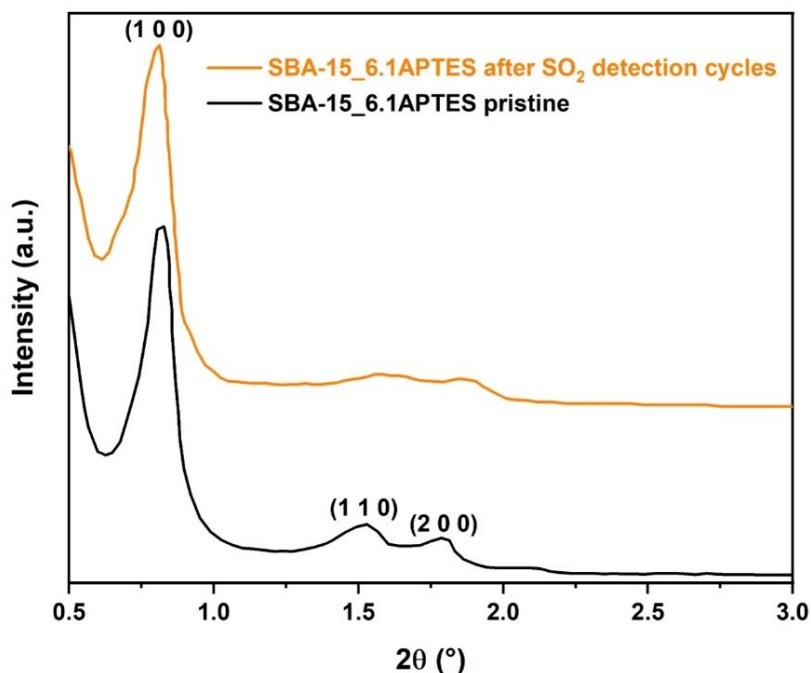


Figure S15. PXRD pattern of SO_2 -saturated SBA-15_6.1APTES after fluorescence cycles.

Table S4. Average decay lifetime of fluorescence.

Sample	τ_1 (ns)	a_1	τ_2 (ns)	a_2	τ_3 (ns)	a_3	Fluorescence lifetime (ns)
Pristine	0.8369	0.2875	2.7955	0.3570	9.0328	0.3555	4.4498
Activated	0.7538	0.2972	2.5446	0.3789	8.4757	0.3239	3.9335
SO ₂ -saturated	0.7082	0.3664	2.5621	0.3714	8.2013	0.2622	3.3614

S7. XPS experiments

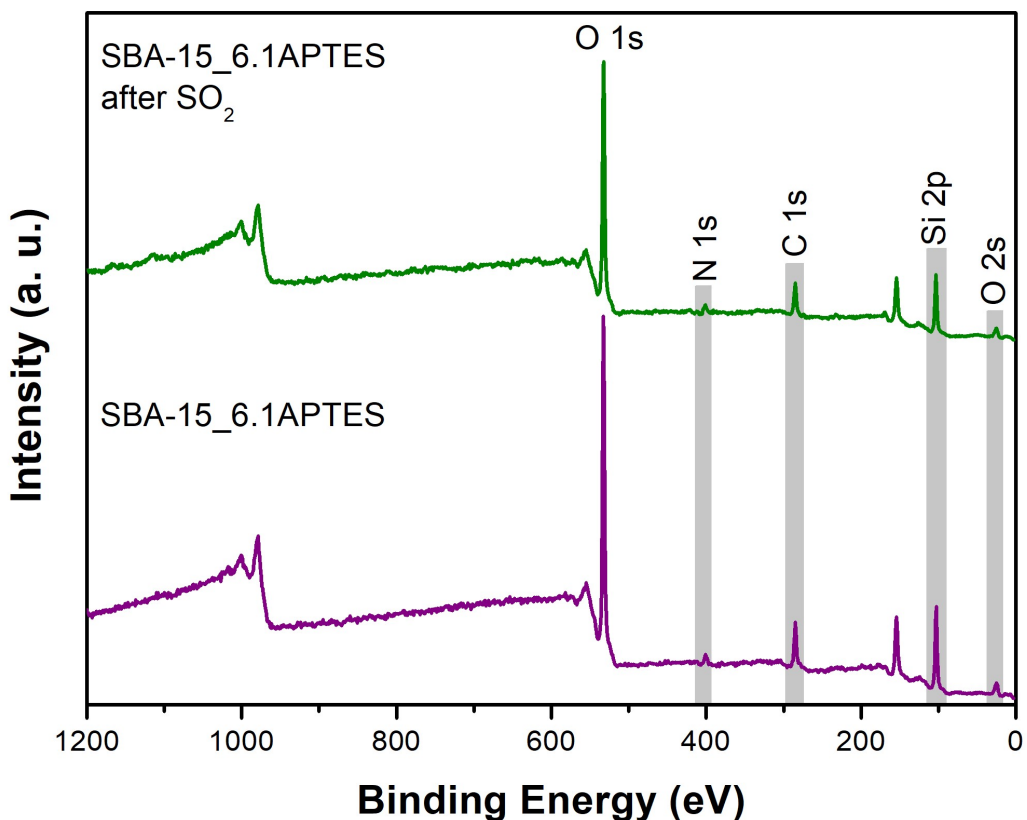


Figure S16. Survey spectra of SBA-15_6.1APTES, before (purple) and after SO₂ exposure (green).

Table S5. The peak-fitting results of C 1s, O 1s, Si 2p and N 1s high-resolution signals.

Sample	Assignment	E_B (eV)	FWHM (eV)	At. %
SBA-15_6.1APTES	C 1s	284.7	1.7	71.1
		286.1	1.7	24.1
		287.5	1.8	4.8
	O 1s	532.4	1.8	-

	Si 2p	103.2	1.9	-
	N 1s	399.7 401.3	2.5 2.5	51.3 48.7
SBA-15_6.1APTES after SO ₂	C 1s	284.8	1.8	68.9
		286.2	1.8	25.9
		287.6	1.8	5.2
	O 1s	532.6	1.9	-
	Si 2p	103.4	1.96	-
	N 1s	399.2	2.4	27.2
		401.7	2.4	72.8

S8. DFT calculations

8.1. Density functional theory Analysis (DFT)

The species (3-Aminopropyl)-triethoxysilane (APTES), SO₂, and the APTES-SO₂ adduct underwent a geometry optimization calculation followed by a frequency calculation using the computational package Gaussian 09, with graphical interpretation via GaussView 6 and USF Chimera 1.17.1. This optimization was performed without constraints to identify the most stable, low-energy structures. The methodology employed the three-parameter hybrid density functional B3LYP alongside a triple- ξ basis set, incorporating diffuse and polarization functions for all atoms, including hydrogen (6-311++g(d,p)). This approach aimed to model changes in electronic density within the molecular environment. Additionally, the same process was carried out using the hybrid long-range-corrected density functional ω B97XD, coupled with a triple- ξ basis set (cc-PVTZ), which already accounts for corrections related to polarization effects, charge transfer, and Van der Waals interactions between molecules.

8.2. DFT results

As can be seen in Table 1, the interaction between APTES and the SO₂ molecule leads to a favorable energy decrease, resulting in a more stable adduct compared to the free species, as expected. The binding energy was determined by calculating the energy difference between the free APTES and SO₂ species and the APTES-SO₂ complex, as follows.

$$E_{binding}(SCF) = E_{Adduct}(SCF) - (E_{APTES}(SCF) + E_{SO_2}(SCF)), \quad (1)$$

where $E_{binding}(SCF)$ is the binding energy between APTES and SO₂ molecules, $E_{Adduct}(SCF)$ is the corrected total electronic energy of the adduct, $E_{APTES}(SCF)$ and $E_{SO_2}(SCF)$ are the corrected total electronic energy of the APTES and SO₂ molecules, respectively. The binding energy was calculated using two different density functionals, B3LYP and ω B97XD, to ensure accuracy and reliability in our results. The binding energies are reported in Table S6.

Table S6. Binding energy calculated using two density functionals.

Binding Energy (kJ/mol)	
B3LYP/6-311++g(d,p)	ω B97XD/cc-PVTZ
-35.0137	-42.9611

The reaction properties were determined according to the following equations for the different state functions.

$$\Delta S_{binding} = \Delta S_{Adduct} - (\Delta S_{APTES} + \Delta S_{SO_2}), \quad (2)$$

$$\Delta H_{binding} = \Delta H_{Adduct} - (\Delta H_{APTES} + \Delta H_{SO_2}), \quad (3)$$

$$\Delta G_{binding} = \Delta G_{Adduct} - (\Delta G_{APTES} + \Delta G_{SO_2}), \quad (4)$$

where $\Delta S_{binding}$, $\Delta H_{binding}$, $\Delta G_{binding}$ represent the entropy change, enthalpy change, and free energy change in the bond formation between APTES and SO_2 molecules, respectively. The ΔS_{Adduct} , ΔH_{Adduct} , ΔG_{Adduct} are the entropy change, enthalpy change, and the free energy of the adduct APTES- SO_2 , respectively. The ΔS_{APTES} , ΔS_{SO_2} , ΔH_{APTES} , ΔH_{SO_2} , ΔG_{APTES} , ΔG_{SO_2} are the entropy change, enthalpy change, and the free energy of the APTES and SO_2 molecules, respectively. Here, the thermodynamic properties were determined at 298 K and 1 atm. As shown in Table S7. Firstly, an entropic decrease is observed, attributed to the reduction in the number of free molecules in the system due to the adsorption of SO_2 by the SBA-APTES. Similarly, the negative sign in the enthalpy change indicates an exergonic process, as the formation of the APTES- SO_2 adduct leads to a more stable species, releasing energy in the process.

Table S7. Binding entropy, enthalpy, and free energies calculated using the two density functionals.

B3LYP/6-311++g(d,p)	ω B97XD/cc-PVTZ
Binding Entropy (kJ/mol·K)	
-0.125551	-0.153433
Binding Enthalpy (kJ/mol)	
-34.291651	-42.871784
Binding Free Energy (kJ/mol)	

3.119094	2.843416
----------	----------

In the case of the binding free energy (see Table S7), at 298 K, the formation of the adduct is a non-spontaneous process. However, according to the definition of free energy, as shown in Eq. (5), it is evident that as the temperature decreases, the process tends towards spontaneity. This property is highly temperature-dependent and aligns with experimental expectations. As the temperature increases, the kinetic energy of the SO₂ molecules rises, along with their average speed, reducing the likelihood of adsorption by the SBA-APTES material. The Gibbs binding energy ($\Delta G_{binding}$) is given by,

$$\Delta G_{binding} = \Delta H_{binding} - T\Delta S_{binding} , \quad (5)$$

where T is the temperature of the system.

Table S8. Binding entropy, enthalpy, free energy and electronic energy obtained by B3LYP/6-311++g(d,p) density functional.

B3LYP/6-311++g(d,p)					
E _i	APTES	SO ₂	→	Adduct APTES-SO ₂	ΔE _i
Enthalpy (kJ/mol)	-2433140.1	-1440491.2		-3873665.7	-34.2916508
Entropy (kJ/mol·K)	0.661031	0.24890878		0.78438839	-0.12555138
Free Energy (kJ/mol)	-2433337.1	-1440565.4		-3873899.4	3.119093575
Total Energy SCF (kJ/mol)	-2433196.8	-1440501.8		-3873733.6	-35.0136632

Table S9. Binding entropy, enthalpy, free energy and electronic energy obtained by ω B97XD/cc-PVTZ density functional.

ω B97XD/cc-PVTZ					
E _i	APTES	SO ₂	→	Adduct APTES-SO ₂	ΔE _i
Enthalpy (kJ/mol)	-2432700.9	-1440410.6		-3873154.4	-42.871784
Entropy (kJ/mol·K)	0.62575971	0.24815512		0.72048221	-0.1534326
Free Energy (kJ/mol)	-2432887.4	-1440484.5		-3873369	2.84341611

Total Energy SCF (kJ/mol)	-2432755.2	-1440421.1		-3873219.3	-42.961051
------------------------------	------------	------------	--	------------	------------

3. Binding distance

Once we obtained the optimized geometries of the APTES-SO₂ adduct, we calculated the interaction distance between the (-NH₂) and (SO₂) functional groups (see Table S10). As shown in Figs. S17 and S18, the sulfur atom of the SO₂ molecule is oriented towards the free electron pair of the nitrogen atom in SBA-15 APTES. In this conformation, the hydrogen atoms are positioned far from the sulfur atom of the SO₂ molecule."

Table S10. Binding distances calculated using the two density functionals.

Binding distances N-S (Å)	
B3LYP/6-311++g(d,p)	ω B97XD/cc-PVTZ
2.514	2.503

In Figs. S17 and S18, the APTES-SO₂ adducts calculated with B3LYP/6-311++G(d,p) and ω B97XD/cc-PVTZ are shown, respectively.

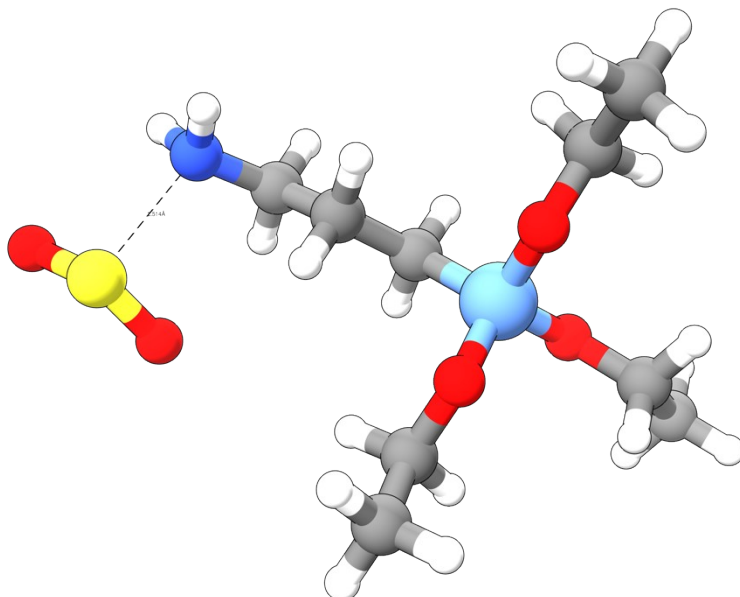


Fig. S17. APTES-SO₂ adduct optimized interaction geometry calculated with B3LYP/6-311++G(d,p) density functional.

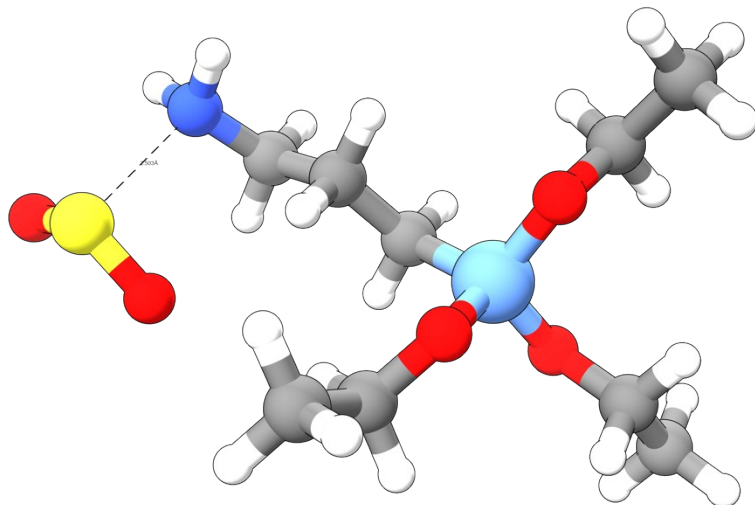


Fig. S18. APTES-SO₂ adduct optimized interaction geometry calculated with ω B97XD/cc-PVTZ density functional.

Finally, based on the Mulliken population analysis for density charge, it is proposed that the APTES-SO₂ interaction primarily occurs through dipole-dipole interactions, predominantly involving the sulfur and nitrogen atoms. The nitrogen atom in APTES exhibits a partially negative charge, while the sulfur atom in SO₂ exhibits a partially positive charge, as depicted in Fig. S19. This does not exclude the possibility of hydrogen bonds but suggests that they play a lesser role in the intermolecular interaction.

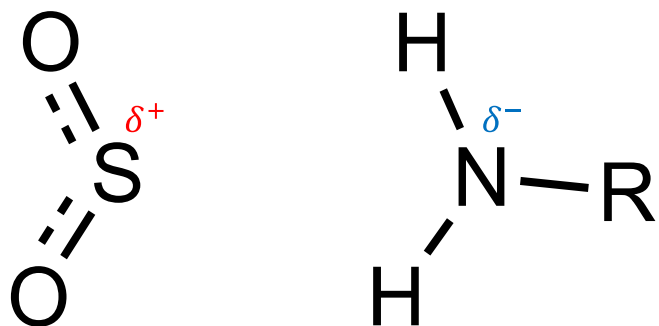


Fig. S19. Predominant interaction diagram between sulfur and nitrogen atoms in the APTES-SO₂ adduct.

Table S11. Nomenclature employed and reported in the present research.

- $E_{binding}(SCF)$: is the binding energy between APTES and SO₂ molecules.
- $E_{Adduct}(SCF)$: is the corrected total electronic energy of the adduct APTES-SO₂.
- $E_{APTES}(SCF)$: is the corrected total electronic energy of the APTES molecule.
- $E_{SO_2}(SCF)$: is the corrected total electronic energy of the SO₂ molecule.
- $\Delta S_{binding}$: is the entropy change in bond formation between APTES and SO₂ molecules.
- $\Delta H_{binding}$: is enthalpy change in bond formation between APTES and SO₂ molecules.
- $\Delta G_{binding}$: is the free energy change in bond formation between APTES and SO₂ molecules.
- ΔS_{Adduct} : is the entropy of the adduct APTES-SO₂.
- ΔH_{Adduct} : is the enthalpy of the adduct APTES-SO₂.
- ΔG_{Adduct} : is the free energy of the adduct APTES-SO₂.
- ΔS_{APTES} : is the entropy of the APTES molecule.
- ΔH_{APTES} : is the enthalpy of the APTES molecule.
- ΔG_{APTES} : is the free energy of the APTES molecule.
- ΔS_{SO_2} : is the entropy of the SO₂ molecule.
- ΔH_{SO_2} : is the enthalpy of the SO₂ molecule.
- ΔG_{SO_2} : is the free energy of the SO₂ molecule.

Table S12. Mulliken population analysis of the two density functionals.

Mulliken population analysis of the adduct			Mulliken population analysis of the adduct		
B3LYP/6-311++G(d,p)			ω B97XD/cc-PVTZ		
1	C	-0.205127	1	C	0.001363
2	C	-0.477031	2	C	-0.248864
3	O	-0.349271	3	O	-0.319283
4	Si	1.310709	4	Si	0.564489
5	C	-1.109451	5	C	-0.342719
6	C	0.229241	6	C	-0.201672
7	C	-0.756589	7	C	-0.109701
8	N	-0.407926	8	N	-0.306979
9	O	-0.287389	9	O	-0.329394
10	C	-0.119303	10	C	0.008309
11	C	-0.480523	11	C	-0.250043
12	O	-0.379518	12	O	-0.319429
13	C	-0.262711	13	C	-0.01409

14	C	-0.459777	14	C	-0.252364
15	H	0.138977	15	H	0.070575
16	H	0.1535	16	H	0.076587
17	H	0.150451	17	H	0.091487
18	H	0.132762	18	H	0.076672
19	H	0.144306	19	H	0.08869
20	H	0.180712	20	H	0.116826
21	H	0.197655	21	H	0.128408
22	H	0.201235	22	H	0.126328
23	H	0.133833	23	H	0.107444
24	H	0.1508	24	H	0.100741
25	H	0.248419	25	H	0.116736
26	H	0.234949	26	H	0.142252
27	H	0.302562	27	H	0.156715
28	H	0.145818	28	H	0.073291
29	H	0.159612	29	H	0.078672
30	H	0.144109	30	H	0.089097
31	H	0.150002	31	H	0.086675
32	H	0.137385	32	H	0.078848
33	H	0.180646	33	H	0.089197
34	H	0.150935	34	H	0.081665
35	H	0.145	35	H	0.089992
36	H	0.137444	36	H	0.083893
37	H	0.146573	37	H	0.091151
38	S	0.489966	38	S	0.692174
39	O	-0.317395	39	O	-0.405842
40	O	-0.28559	40	O	-0.407899
Total Charge	Sum	0.000	Total Charge	Sum	0.000

Table S13. Optimized geometry of SO₂.

SO ₂ optimized geometry				
B3LYP/6-311++G(d,p)				
1	S	0.00000	0.00000	0.37171
2	O	0.00000	1.25449	-0.37171
3	O	0.00000	-1.25449	-0.37171

Table S14. Optimized geometry of APTES.

APTES optimized geometry				
B3LYP/6-311++G(d,p)				
1	C	-0.50385	-2.66155	0.65446
2	C	-0.55155	-3.49639	1.92277
3	O	-0.50712	-1.27904	1.00623
4	Si	-0.40693	0.00439	-0.03190
5	C	1.13180	-0.02159	-1.09530
6	C	2.46334	-0.00500	-0.32347
7	C	3.68436	-0.04055	-1.24445
8	N	4.92799	0.02833	-0.46734
9	O	-1.67127	0.01949	-1.10671
10	C	-3.06400	0.04935	-0.77938
11	C	-3.87873	0.02065	-2.06074
12	O	-0.47017	1.28984	1.00422
13	C	-0.39018	2.67203	0.65701
14	C	-0.44184	3.50582	1.92560
15	H	0.40016	-2.90171	0.07900
16	H	-1.36794	-2.88816	0.01694
17	H	-1.45433	-3.27113	2.49517
18	H	-0.55165	-4.56264	1.67687
19	H	0.31467	-3.28407	2.55357
20	H	1.07742	-0.90606	-1.74276
21	H	1.08215	0.83592	-1.77829
22	H	2.53261	0.88629	0.30765

23	H	2.50785	-0.86161	0.36076
24	H	3.61926	-0.93159	-1.89089
25	H	3.65892	0.83064	-1.90793
26	H	5.03571	-0.79583	0.11609
27	H	5.73854	0.07120	-1.07591
28	H	-3.31448	-0.81058	-0.14649
29	H	-3.28855	0.95502	-0.20322
30	H	-3.63917	0.88248	-2.68822
31	H	-3.66784	-0.88725	-2.63105
32	H	-4.94832	0.04536	-1.83130
33	H	0.54348	2.86976	0.11440
34	H	-1.22083	2.93907	-0.00878
35	H	0.39231	3.25246	2.58371
36	H	-0.38352	4.57115	1.68282
37	H	-1.37305	3.32247	2.46668

Table S15. Optimized geometry of the adduct APTES-SO₂.

Adduct APTES-SO ₂ optimized geometry				
B3LYP/6-311++G(d,p)				
1	C	2.73600	2.48400	0.50600
2	C	3.15100	3.28800	1.72600
3	O	2.15300	1.25300	0.93500
4	Si	1.61400	0.03200	-0.04200
5	C	0.17600	0.55100	-1.12600
6	C	-1.05400	1.04500	-0.34700
7	C	-2.23700	1.36300	-1.26000
8	N	-3.42400	1.73400	-0.47200
9	O	2.78900	-0.48000	-1.09200
10	C	4.06200	-1.03300	-0.73700
11	C	4.69800	-1.65500	-1.96700

12	O	1.20000	-1.13700	1.04600
13	C	0.57500	-2.39100	0.75100
14	C	0.38200	-3.16400	2.04300
15	H	2.01100	3.05300	-0.09200
16	H	3.60400	2.28600	-0.13400
17	H	3.88200	2.73300	2.31900
18	H	3.60000	4.23800	1.42000
19	H	2.28700	3.49900	2.35900
20	H	0.52600	1.32100	-1.82500
21	H	-0.10000	-0.30800	-1.75000
22	H	-1.36800	0.28600	0.37600
23	H	-0.79300	1.93800	0.23500
24	H	-1.96200	2.15400	-1.97100
25	H	-2.49800	0.47300	-1.84100
26	H	-3.20800	2.42300	0.24200
27	H	-4.17600	2.09900	-1.05000
28	H	4.70300	-0.23900	-0.33500
29	H	3.93500	-1.78200	0.05300
30	H	4.07100	-2.45900	-2.36000
31	H	4.82900	-0.90700	-2.75300
32	H	5.67900	-2.07100	-1.71800
33	H	-0.39300	-2.21900	0.26500
34	H	1.20000	-2.96200	0.05300
35	H	-0.24800	-2.60200	2.73500
36	H	-0.09800	-4.12600	1.83900
37	H	1.34300	-3.35000	2.52800
38	S	-4.57000	-0.34400	0.35800
39	O	-5.86400	-0.04500	-0.26900
40	O	-3.68900	-1.27500	-0.36400

Table S16. Optimized geometry of SO₂.

SO ₂ optimized geometry				
ω B97XD/cc-PVTZ				
1	S	0.00000	0.00000	0.36876
2	O	0.00000	1.23414	-0.36876
3	O	0.00000	-1.23414	-0.36876

Table S17. Optimized geometry of APTES.

APTES optimized geometry				
ω B97XD/cc-PVTZ				
1	C	-0.73394	-2.56968	0.57822
2	C	-1.11826	-3.42438	1.76586
3	O	-0.56317	-1.23273	1.00511
4	Si	-0.36769	0.02289	-0.03399
5	C	1.16170	-0.13941	-1.08007
6	C	2.45851	-0.12402	-0.26776
7	C	3.69487	-0.33579	-1.12811
8	N	4.90742	-0.24525	-0.32269
9	O	-1.62719	0.11992	-1.08873
10	C	-2.97662	0.27093	-0.68374
11	C	-3.87182	0.20031	-1.90091
12	O	-0.32170	1.31597	0.97223
13	C	-0.11939	2.64325	0.52879
14	C	-0.18200	3.57617	1.71790
15	H	0.19607	-2.94158	0.13339
16	H	-1.50873	-2.62460	-0.19447
17	H	-2.04731	-3.06361	2.20613
18	H	-1.25604	-4.46259	1.46186
19	H	-0.34138	-3.38441	2.52848
20	H	1.08343	-1.06881	-1.65311
21	H	1.16887	0.66425	-1.82184

22	H	2.56547	0.82334	0.26444
23	H	2.42271	-0.90071	0.50272
24	H	3.59114	-1.29012	-1.66484
25	H	3.73567	0.44757	-1.88886
26	H	4.93040	-0.99399	0.35751
27	H	5.72927	-0.35295	-0.90094
28	H	-3.24389	-0.51328	0.03211
29	H	-3.10387	1.23104	-0.17368
30	H	-3.60502	0.98028	-2.61344
31	H	-3.76545	-0.76482	-2.39566
32	H	-4.91616	0.33202	-1.61608
33	H	0.85550	2.73074	0.03569
34	H	-0.88307	2.91540	-0.20799
35	H	0.58412	3.31109	2.44551
36	H	-0.02339	4.60822	1.40366
37	H	-1.15445	3.50419	2.20398

Table S18. Optimized geometry of the adduct APTES-SO₂.

Adduct APTES-SO ₂ optimized geometry				
ω B97XD/cc-PVTZ				
1	C	3.01200	2.17500	0.39300
2	C	3.71700	2.90000	1.51800
3	O	2.27900	1.09000	0.92400
4	Si	1.56700	-0.05200	-0.01800
5	C	0.20800	0.63900	-1.09000
6	C	-0.96600	1.17600	-0.27100
7	C	-2.15100	1.56800	-1.13700
8	N	-3.30800	1.89900	-0.30500
9	O	2.65800	-0.72000	-1.05000

10	C	3.83200	-1.39200	-0.62600
11	C	4.64200	-1.79300	-1.83900
12	O	0.99200	-1.12400	1.07600
13	C	0.09500	-2.17800	0.76700
14	C	-0.69100	-2.54700	2.00500
15	H	2.33600	2.86100	-0.13000
16	H	3.74100	1.81700	-0.34300
17	H	4.40900	2.22900	2.02700
18	H	4.27800	3.75100	1.13100
19	H	2.99400	3.26100	2.24800
20	H	0.61800	1.41600	-1.74000
21	H	-0.13600	-0.15700	-1.75600
22	H	-1.30000	0.41900	0.44100
23	H	-0.64300	2.03800	0.32000
24	H	-1.87500	2.39300	-1.80200
25	H	-2.43200	0.72100	-1.76900
26	H	-3.05600	2.52900	0.44600
27	H	-4.05400	2.32200	-0.84100
28	H	4.42200	-0.74000	0.02600
29	H	3.55900	-2.27600	-0.04100
30	H	4.05700	-2.44700	-2.48600
31	H	4.92900	-0.91200	-2.41300
32	H	5.54700	-2.32000	-1.53600
33	H	-0.59900	-1.88000	-0.02600
34	H	0.66300	-3.04000	0.40300
35	H	-1.26900	-1.69100	2.35200
36	H	-1.38300	-3.36000	1.78300
37	H	-0.02000	-2.86100	2.80400
38	S	-4.43100	-0.26500	0.26200
39	O	-5.46300	-0.08700	-0.73500
40	O	-3.32300	-1.11800	-0.11700

S9. References

1. C. M. Simon, B. Smit, M. Haranczyk, *Comput. Phys. Commun.* **2016**, *200*, 364–380.
2. J. L. Obeso, V. B. López-Cervantes, R. Ojeda-López, A. Yañez-Aulestia, S. Cordero-Sánchez, E. Sánchez-González, O. Novelo-Peralta, K. E. Reyes Morales, D. Solís-Ibarra, I. A. Ibarra and J. M. Esparza-Schulz, *Ind Eng Chem Res*, **2024**, *63*, 2223–2230.
3. P. Brandt, A. Nuhnen, S. Öztürk, G. Kurt, J. Liang, C. Janiak, C, *Adv. Sustain. Syst.*, **2021**, *5*, 2000285.
4. X. Cui, Q. Yang, L. Yang, R. Krishna, Z. Zhang, Z. Bao, H. Wu, Q. Ren, W. Zhou, B. Chen, H. Xing, *Adv. Mater.*, **2017**, *29*, 1606929.
5. A. Nuhnen, C. Janiak, *Dalt. Trans.*, **2020**, *49*, 10295–10307.
6. J-G. Shim, Y. H. Jhon, j-H. Kim, K-R. Jang, and J. Kim, *Bull. Korean Chem. Soc.* **2007**, Vol. 28, No. 9 1609.
7. R. Steudel and Y. Steudel, *Eur. J. Inorg. Chem.* **2007**, 4385–4392.